Scientia Iranica B (2014) 21(6), 1907–1919

Sharif University of Technology
Scientia Iranica
Transactions B: Mechanical Engineering
www.scientiairanica.com

3D kinematics of cylindrical nanoparticle manipulation by an atomic force microscope based nanorobot

M.H. Korayem[a,b,*] and A.K. Hoshiar[a]

a. *Department of Mechanical and Aerospace Engineering, Science and Research Branch, Islamic Azad University, Tehran, Iran.*
b. *Robotic Research Laboratory, Center of Excellence in Experimental Solid Mechanics and Dynamics, School of Mechanical Engineering, Iran University of Science and Technology, Tehran, Iran.*

Received 18 December 2012; received in revised form 28 October 2013; accepted 28 July 2014

KEYWORDS
Manipulation;
Cylindrical nanoparticle;
AFM nanorobot;
3D kinematics.

Abstract. In recent years, the positioning of cylindrical nanoparticles, like CNTs and nanowires, by means of Atomic Force Microscope (AFM) nanorobots has been investigated widely. Despite this growing scientific interest, no one has studied 3D model simulations of different modes (sliding, rolling and rotation). Previous work has only focused on two-dimensional simulations, which often cannot be extended to the manipulation of cylindrical particles. The aim of this study is to present a 3D model for the positioning of cylindrical nanoparticles. In order to validate the results, 2D and 3D simulations have been compared. Moreover, the findings show that both simulations act similarly with a gradual decrease in the effects of 3D parameters. We have developed a 3D kinematic model, which makes it possible to predict the positioning process from the moment the tip of the cantilever touches the particle to when the particle reaches the desired point. These simulations also determine the displacements of the particle and cantilever during the time when the particle is stuck into the substrate. In response to real-time monitoring limitations, the introduced kinematic simulation is able to predict the motion behavior of a cylindrical nanoparticle during the manipulation process.

1. Introduction

The manipulation of nanoparticles by AFM has been studied ever since the AFM instrument was invented. The AFM's cantilever tip can be used for particle moving, writing, cutting or surface touching in nano scale. In recent years, the positioning of nanoparticles and the manufacturing of nano-scale structures has been studied in much research work. The term 'manipulation' has come to refer to the pushing process of nanoparticles by AFM robots. In the manipulation process, the cantilever tip touches the particle, and because of the motion of the cantilever and substrate, the particle is pushed toward a desired position (Figure 1).

The attractiveness of real-time monitoring, on the one hand, and the necessity of improving the automation process, on the other, are the motives behind many research papers that have been published on the modeling and simulation of nanoparticle positioning [1-3]. The existing models have been developed for 2D manipulation processes, like the positioning of spherical nanoparticles [4]. The increasing use of the cylindrical nanoparticle manipulation process in the manufacturing of nanostructures has prompted the present work [5,6]. We have tried to present a model for predicting cylindrical particle motion behavior.

Computational simulations for prediction of the motion behavior of nanoparticles have received much attention over the past decade [7]. In the computa-

*. *Corresponding author. Tel.: +98 2144865239; Fax: +98 21 44865239*
E-mail addresses: Hkorayem@iust.ac.ir (M.H. Korayem); A_k_hoshiar@yahoo.com (A.K. Hoshiar)

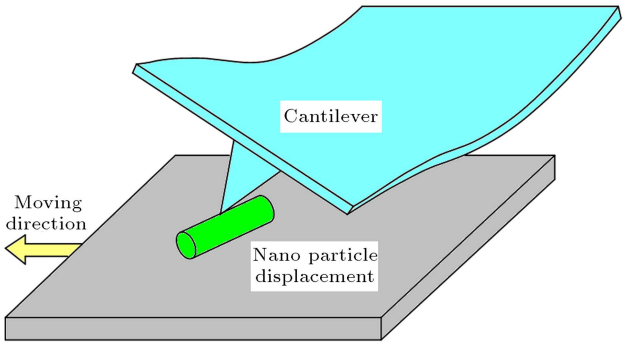

Figure 1. Manipulation (pushing) of a cylindrical nanoparticle by AFM nanorobot.

tional method, particle position can be found using a force-time diagram [8]. Due to the complex modes of motion displayed by cylindrical nanoparticles, the modeling and simulation of cylindrical nanoparticle positioning has been pursued less often than other aspects of this field.

The process of nanoparticle manipulation has been gaining increased interest due to the improved use of AFM in particle positioning [9]. Junno was one of the first to demonstrate a method for controlled particle positioning [10]. In [11,12], the authors studied the mechanical characteristics of cylindrical nanoparticles using the AFM based manipulation process. The first investigations into the moving of CNT particles by the Atomic Force Microscope found that there are different motion modes, like sliding and rolling, in the process [8]. Several studies (e.g. [6,13,14]) have concentrated on the subject of nanowire positioning. Research has tended to focus on experimental methods rather than practical approaches [15]. The problem with experimental methods is that they are not repeatable, the process is not automatic, and a precise manufacturing capability does not exist. Therefore, this paper has presented the modeling of the nanomanipulation process for a controlled and precise operation, which is repeatable.

What is known about controlled particle manipulation processes using AFM nanorobots is largely based on the works of Sitti and Hashimoto. In their cutting edge article, they proposed a dynamic model for the manipulation of spherical nanoparticles [7]. They modified this model in subsequent work to include the motion mode, and obtained the time and force relations in a 2D spherical nanoparticle positioning process [16,17]. Korayem et al. has suggested a dynamic model for this process, based on coupled equations, which seems to be a reliable approach. Also, because of the real-time monitoring obstacle, he has proposed an algorithm to find the maximum size of particles that can be manipulated [4,18]. The effect of tip position in rectangular and V-shaped cantilevers has been investigated, and sensitivity analyses of effective parameters have been presented by Korayem et al. [19,20]. In the manipulation of spherical nano particles, the process is conducted in one direction (X) and the other direction (Z) mainly remains constant during the process. However, in cylindrical nano particle manipulation (especially in rotation mode), the process is conducted in 2 directions (X and Y), and the third direction (Z) is mainly considered as constant. The major shortcoming of these models is that they are restricted to 2D simulations (X and Z directions) that only cover the manipulation of spherical particles.

Zhang reported a new method for the manipulation of nanowires using a particular cantilever [21]. A nanowire manipulation process that considers the ratio effect was presented [22]. In the most recent work, a dynamic model has been proposed to clarify the dynamic forces in manipulation of a cylindrical nano particle [23]. In published research work, so far, no 3D model capable of simulating the kinematics of sliding, rolling and rotation modes has been presented. The rotation mode, which has been widely observed in experimental research, is neglected in 2D models [24]. So, at this point, a complete modeling, which is able to demonstrate all the possible modes, is greatly needed. In this work, a comprehensive model to describe the kinematics of cylindrical nano particle manipulation in different modes is presented.

This paper investigates the kinematics of the 3D modeling of cylindrical nanoparticle manipulation, including all possible motion modes (sliding, rotating and rolling). The modeling process has been divided into five steps. In each step, the kinematic model is improved based on the effective parameters. In the first step, the cantilever and particle are considered a rigid body, and basic modeling has been introduced. In the second step, for more accurate modeling, the elastic behavior of particles has been introduced. Then, the elastic behavior of the cantilever in XZ and XY plane has been added to the model in the third and fourth steps, respectively. In the final step, the cylindrical particle position in the XY plane is added, and the final model, which contains all possible deformations, has been presented. This model includes variable and constant parameters which are simulated using an algorithm. Applying the proposed algorithm, all possible kinematic modes are investigated and dynamic modes, such as rolling, sliding and rotating, are demonstrated.

This paper is organized as follows. In the first section, a kinematic model is presented, which shows the motion and acceleration variations during the manipulation process. This model is also able to demonstrate the elastic behavior of the cantilever and nanoparticle. In the second section, the relevant contact model is developed. In the third section, an algorithm-based simulation is introduced. These

simulations also show the particle positioning process in different modes. A verification method based on the elimination of 3D parameters is outlined in the fourth section.

2. Kinematic modeling of the manipulation of cylindrical nano particles

Many experts now contend that the main obstacle in the manipulation of a nanoparticle using the AFM nanorobot is particle shape. Therefore, it might be more appropriate to formulate the kinematics and dynamics of the process in 3D form [7,16,17,22]. In order to properly study the cylindrical particle manipulation, the kinematic model should be improved. The growing use of cylindrical nanoparticles in MEMS and NEMS has motivated us to find a kinematic model that is able to demonstrate the particle positioning process.

With the change in particle shape, a different contact model should be applied. In an attempt to simulate cylindrical contact, an improved contact model has been developed. Therefore, the presented kinematic model comprises the particle positioning and the improved contact model. The modeling process is based on a progressive method that incorporates effective parameters at each step. Finally, a 3D model encompassing all the possible conditions is introduced.

The following assumptions have been considered in the modeling process:

1. Modeling variables (γ, θ) are employed up to the point where the particle stops in the substrate. Moreover, during the positioning process, the parameters are applied as constants.
2. The cantilever deformation is assumed to be formulated in several steps. In other words, all effective parameters are not applied at once, but a progressive formulation method is used for this purpose.

The proposed modeling scheme integrates all effective parameters into the model in five steps. In the first step, a model is introduced with no deformation in the cantilever and particle, which is accepted as a solid state model with no deformation. Then, with the application of contact mechanics, the particle and deformation are incorporated into the model. In the next step, cantilever deformation effects, which are modeled by 2 variables (γ, θ), are added to the model. Finally, the rotation angle related to the rotation mode is integrated into the model, and the modeling process is completed.

Step one: The model is supposed to be in solid state. So, it does not exhibit any elastic deformation. Therefore, using a fixed coordinate system, as shown in Figure 2, the kinematic equation is introduced. In the presented models for the contact of probe tip and particle, an angle which is assumed to be constant is introduced as (ϕ). The axis is demonstrated with X, Y, and Z. The position of the reference point is defined by the X_p, Y_p and Z_p components (Figure 2), R_p is the particle's radius. It is obvious that both of the demonstrated origins coincide. So, there is no distance between these origins, and parameters (X_s, Z_s) are assumed to be zero.

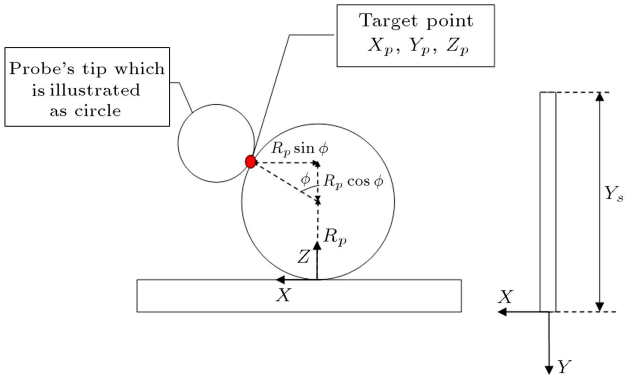

Figure 2. Step one: Particle-probe relation in solid state.

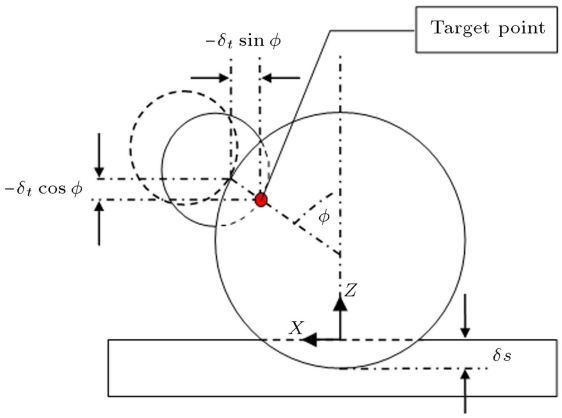

Figure 3. Step two: Particle-probe relation in elastic state.

Step two: Elastic deformation occurs in the tip and particle and also in the surfaces of the substrate and particle. In the improved elastic model, some changes have been made to particle positions, which are shown in Figure 3. These changes are used in the model for one step improvement. In the related equations, elastic deformation in the probe tip and particle is indicated by δ_t, and contact between the particle and substrate is indicated by δ_s. The rest of the parameters are similar to the previous step. Eventually, the first and second steps are used in Eq. (1):

$$X_p = X_s + R_p \sin\phi - \delta_t \sin\phi,$$

$$Z_p = Z_s + R_p + R_p \cos\phi - \delta_t \cos\phi - \delta_s,$$

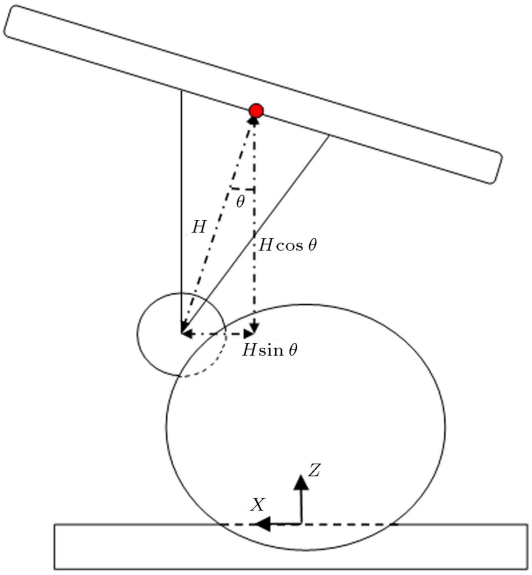

Figure 4. Step three: Considering the cantilever's twist angle (θ) in the modeling process.

$$Y_p = Y_s. \tag{1}$$

Step three: Cantilever deformation, which plays a major role in the manipulation process, has not been mentioned. The forces exerted during manipulation move the cantilever up and twist it. A bending also occurs in the cantilever. The target point changes and the cantilever deformation is integrated into the formulation. Cantilever deformation has been illustrated in Figure 4, where θ denotes the twist angle (an angle in the XZ plane and caused by the force in the X direction (Figure 4)). The position of the probe's height is defined by H in Figure 4. The model is improved by means of the twist angle. The following equation is proposed to express the position of the target point:

$$X_p = X_s + (R_p - \delta_t)\sin\phi - H\sin\theta,$$

$$Z_p = Z_s + (R_p - \delta_t)\cos\phi + (R_p - \delta_s) + H\cos\theta,$$

$$Y_p = Y_s. \tag{2}$$

Step four: Cantilever deformation has been shown in Figure 5, where γ indicates the bending of the cantilever, γ (an angle in the ZY plane and caused by the force in the Y direction (Figure 5)); O is the contact point between the probe tip and particle; and H is the probe height. The kinematic model has been improved using the target point in Figure 5. Based on geometrical relations, the length of line AB is equal to $2H\sin(\frac{\gamma}{2})$. Therefore, AE's length equals $2H\sin(\frac{\gamma}{2})\cos(\frac{\gamma}{2})$ and EB's length equals $2H\sin^2(\frac{\gamma}{2})$. By integrating AE and EB into the equations, a more accurate model is achieved.

$$X_p = X_s + (R_p - \delta_t)\sin\phi - H\sin\theta,$$

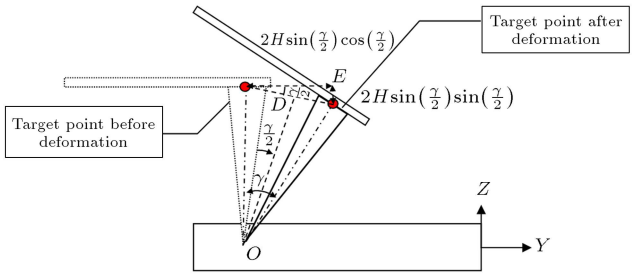

Figure 5. Step four: Considering the cantilever's bending angle (γ) in the modeling process.

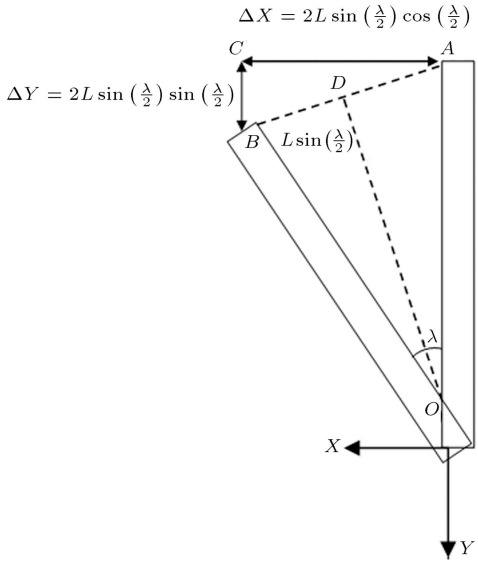

Figure 6. Step five: Considering the rotation of nanoparticle (λ) in the modeling process.

$$Z_p = Z_s + (R_p - \delta_t)\cos\phi + (R_p - \delta_s) + H\cos\theta - 2H\sin^2\left(\frac{\gamma}{2}\right),$$

$$Y_p = Y_s + 2H\sin\left(\frac{\gamma}{2}\right)\cos\left(\frac{\gamma}{2}\right). \tag{3}$$

Step five: The cylindrical nanoparticle's rotation is incorporated into the kinematic equation. The rotation angle has been illustrated in Figure 6 where λ denotes the spin angle (an angle in the XY plane that demonstrates the rotating mode in manipulation of the cylindrical nano particle (Figure 6)). L is the particle length. A, B and D are used to describe the modeling process, and O is the origin of the axis. ΔX and ΔY are displacements in X and Y directions, as a result of rotation. Based on geometrical relations, the length of line AB is equal to $2L\sin(\frac{\lambda}{2})$, with L standing for the length of the nanoparticle. Obviously, the lengths of lines AC and BC are equal to $2L\sin(\frac{\lambda}{2})\cos(\frac{\lambda}{2})$ and $2L\sin^2(\frac{\lambda}{2})$, respectively. By obtaining the new relations, the modeling process is completed. The 3D kinematic equation, which is capable of expressing nanoparticle positioning in 3 dimensions, is ultimately

represented by Eq. (4):

$$\begin{aligned} X_p =& X_s + (R_p - \delta_t)\sin\phi - H\sin\theta \\ &+ 2L\sin\left(\frac{\lambda}{2}\right)\cos\left(\frac{\lambda}{2}\right), \\ Z_p =& Z_s + (R_p - \delta_t)\cos\phi + (R_p - \delta_s) + H\cos\theta \\ &- 2H\sin^2\left(\frac{\gamma}{2}\right), \\ Y_p =& Y_s + 2H\sin\left(\frac{\gamma}{2}\right)\cos\left(\frac{\gamma}{2}\right) + 2L\sin^2\left(\frac{\lambda}{2}\right). \end{aligned} \quad (4)$$

In the final step of the process, the particle acceleration during the nanomanipulation process is determined by taking the second derivative of the kinematic equation. Taking into account the variable parameters of θ, λ, γ, δ_t and δs, the final equation is expressed as:

$$\begin{aligned} \ddot{X}_p =& -\ddot{\delta}_t\sin\phi - H\ddot{\theta}\cos\theta + H\dot{\theta}^2\sin\theta \\ &+ L\ddot{\lambda}\cos^2\left(\frac{\lambda}{2}\right) - L\dot{\lambda}^2\cos\left(\frac{\lambda}{2}\right)\sin\left(\frac{\lambda}{2}\right) \\ &- L\ddot{\lambda}\sin^2\left(\frac{\lambda}{2}\right) - L\dot{\lambda}^2\sin\left(\frac{\lambda}{2}\right)\cos\left(\frac{\lambda}{2}\right), \\ \ddot{Z}_p =& -\ddot{\delta}_t\cos\phi - \ddot{\delta}_s - H\ddot{\theta}\sin\theta - H\dot{\theta}^2\cos\theta \\ &- 2H\ddot{\gamma}\sin\left(\frac{\gamma}{2}\right)\cos\left(\frac{\gamma}{2}\right) - H\dot{\gamma}^2\cos^2\left(\frac{\gamma}{2}\right) \\ &+ H\dot{\gamma}^2\sin^2\left(\frac{\gamma}{2}\right), \\ \ddot{Y}_p =& H\ddot{\gamma}\cos^2\left(\frac{\gamma}{2}\right) - H\ddot{\gamma}\sin^2\left(\frac{\gamma}{2}\right) \\ &- 2H\dot{\gamma}^2\sin\left(\frac{\gamma}{2}\right)\cos\left(\frac{\gamma}{2}\right) \\ &+ 2L\ddot{\lambda}\sin\left(\frac{\lambda}{2}\right)\cos\left(\frac{\lambda}{2}\right) \\ &+ L\dot{\lambda}^2\cos^2\left(\frac{\lambda}{2}\right) - L\dot{\lambda}^2\sin^2\left(\frac{\lambda}{2}\right). \end{aligned} \quad (5)$$

Thus, the equations that include the positions and accelerations in the manipulating process have been obtained. In the next phase, the deformation relations shall be determined.

3. Modeling the elastic deformations in contact areas

Based on Eqs. (4) and (5), manipulation kinematics has a relationship with the particle's elastic deformation. The JKR contact model has been employed in the modeling process [7,16-17]. This model is the improved version of the Hertz model, with applications in the nano scale [25]. Elastic deformation has been applied in the Hertz model, and, in the JKR model, the adhesive effect has been integrated into the modeling [26-28]. To consider the sticking effect in the nano scale, the JKR model is used in the modeling process.

The contact model for cylindrical particles is divided into two parts. The first part of the model shows contact between the probe and particle and the second part depicts contact between the particle and substrate. A sphere-sphere contact is assumed between the particle and probe. The contact area between the tip and particle is not longitudinal; consequently, the cylinder's length has no role in the modeling process. The contact between the nanocylinder and the substrate is assumed as being between two cylinders.

In the first step, the JKR model for tip-particle contact is developed. Using the JKR contact model, the same deformation equation as proposed by Tafazzoli [16,17] is obtained:

$$a^3 = \frac{3R}{4K}\left(F + 3\omega\pi R + \sqrt{6\omega\pi RF + (3\omega\pi R)^2}\right), \quad (6)$$

$$\delta = \frac{a^2}{R'} - \frac{2}{3}\sqrt{\frac{3\pi\omega a}{K}}. \quad (7)$$

In this equation, F stands for the normal force applied on the contact surface, and ω denotes the surface energy. If the surface energy is excluded from the model, it will act as the Hertz model. In the presented equations, K denotes the equivalent modulus of elasticity and R is the particle and probe tip equivalent radiuses, which are determined by the following equations:

$$K = \left(\frac{1-\upsilon_1}{E_1} + \frac{1-\upsilon_2}{E_2}\right), \quad (8)$$

$$R = \frac{R_1R_2}{R_1+R_2}. \quad (9)$$

The particle deformation due to tip-particle contact has been formulated by Eqs. (6) to (9). In the introduced relations, the probe tip is modeled by a sphere with the radius of 20 nm. Therefore, using these equations, it would be possible to model the deformations that are caused by particle-probe contact.

For the modeling of the particle-substrate contact zone, the JKR model for cylindrical nanoparticles has been introduced in Eq. (10). In the presented model, the adhesion forces are based on the JKR model. By excluding the surface energy from the equation, the Hertz model is obtained. As expected, for cylindrical contact, L denotes the length of the nanoparticle.

$$a^3 = \frac{3R}{4K}\left(\frac{16F}{3\pi L}\sqrt{\left(\frac{2FR}{\pi KL}\right)} + 3\gamma\pi R + \sqrt{6\gamma\pi RF + (3\gamma\pi R)^2}\right), \quad (10)$$

$$\delta = \frac{3\pi a^2}{8R}L - \sqrt{\frac{6\pi L^2\omega a}{K}}. \quad (11)$$

The adhesion terms have been modeled by the JKR formulation, and using the presented equations (Eqs. (10) and (11)), the deformation (δ_s), due to applied forces, has been obtained.

4. Kinematic simulation of cylindrical nanoparticle manipulation

An algorithm has been presented for the kinematic simulation process (Figure 7). The kinematic model has been modified based on two assumptions:

1. The substrate speed is constant;
2. The contact angle between the particle and tip is constant during the process.

The model used in the algorithm is obtained by taking these assumptions into consideration.

The constant parameters of the simulation process have been listed in Table 1. The modified simulation model (as shown in the algorithm) is used by incorporating the three variables of F, θ and γ. The deformations are now simulated by applying the JKR model (as shown in Figure 7).

The twist angle (θ), bending angle (γ) and normal forces (F) have been used in the simulation process. At this stage, the particle is stuck into the substrate and it moves with the same constant speed of the substrate. Therefore, 3D deformations occur in the cantilever. The mentioned parameters are assumed to vary within the following intervals: twist angle,

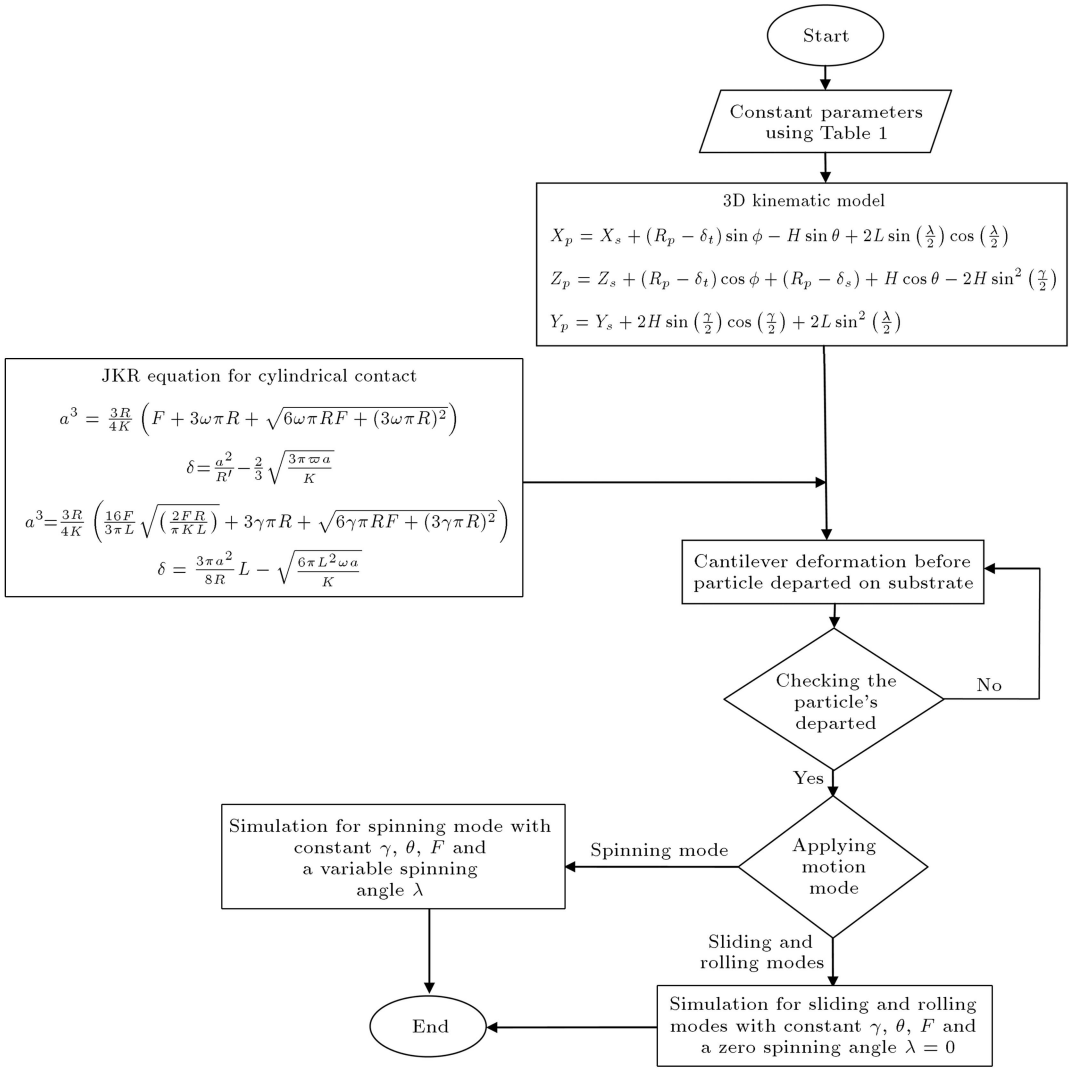

Figure 7. Kinematic simulation algorithm for cylindrical nanoparticle manipulation.

Table 1. Constants for kinematic simulation.

Contact angle ϕ	Equal modulus of elasticity K	Surface adhesion energy ϕ	Substrate speed V_{Stage}	Cantilever height H	Tip radius R_t	Cylindrical particle radius R_P	Nanoparticle length L
45°	5.48×10^9	0.1	10 μm	12 μm	20 nm	100 nm	1000 nm

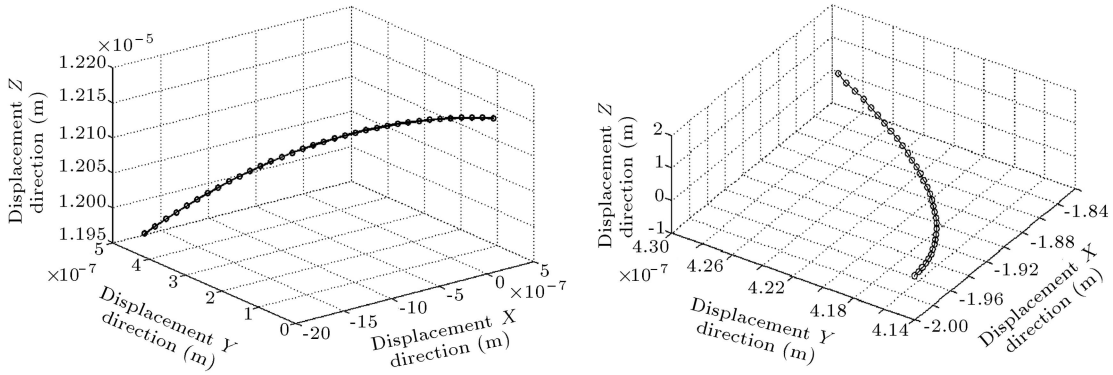

Figure 8. 3D kinematics of the manipulation process before particle's departure (left) and after particle's departure in spinning mode (right).

$0 \leq \theta \leq 10$, bending angle, $0 \leq \gamma \leq 2$, and normal forces, $0 \leq F \leq .1$ μm. Using the formula and applying the constant and variable parameters furnishes the 3D kinematics of the manipulation from the point the tip touches the particle to the point the particle dislodges and departs from the substrate (Figure 8).

At the next stage, the particle dislodges and departs from the surface, instigating the dynamic mode. Regarding the motion modes, two possible outcomes are expected. In cases of sliding and rolling modes, rotation parameter λ is eliminated from the equations, and variables γ, θ and F take on their last values. Thus, one-dimensional linear motion is expected, and the only position change (duo to substrate velocity) is in the x direction.

In the case of spinning mode, rotation parameter λ is a variable. So, 3D kinematics is expected, as shown in Figure 8. Based on the simulation, the particle has a constant motion on the Z-plane. Eventually, using this algorithm, it is possible to demonstrate 3D kinematics during the manipulation process.

The presented simulations demonstrate the 3D kinematics of the manipulation process. At this point, displacements during the process are investigated. Based on the presented formulation and relevant simulations, particle positioning is possible to perform. At this stage, the simulations are divided into three cases:

1. Cantilever deformation and the corresponding particle position;
2. Sliding and rolling modes in the manipulation;
3. Spinning mode during the positioning process.

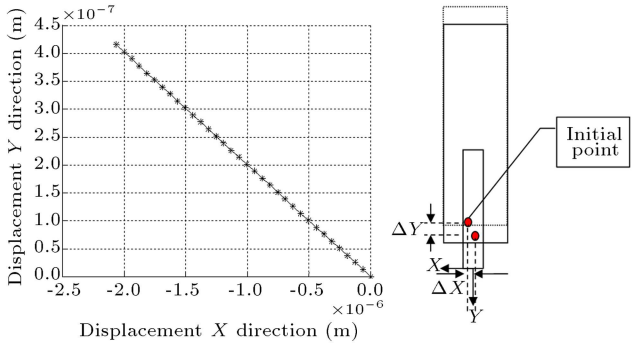

Figure 9. Simulation of target point before departure in X and Y directions.

In the first case, parameters γ and θ are variables (relevant simulations are shown in Figures 9 to 14). In the case of probe deviation, an directions increase in the target point position in the Y direction and a decrease in the target point position in the X direction have been observed (effect of changing the bending angle (γ), Figure 9). Besides, the target point changes position in the Z direction, as shown in Figure 10. The twisting of the cantilever (θ) during the manipulation process results in the decrease of target point position in both X and Z directions (Figures 11 and 12), while it leads to an increase in target point position in the Y direction.

In the case of rolling and sliding modes, one-dimensional displacement occurs in the X direction. The sliding and rolling simulation is presented in Figures 13 and 14. Obviously, no displacement occurs in the Y and Z directions; that is why dots are used in the simulations for no displacement. The only displacement is in the X direction, and it is due to substrate movement.

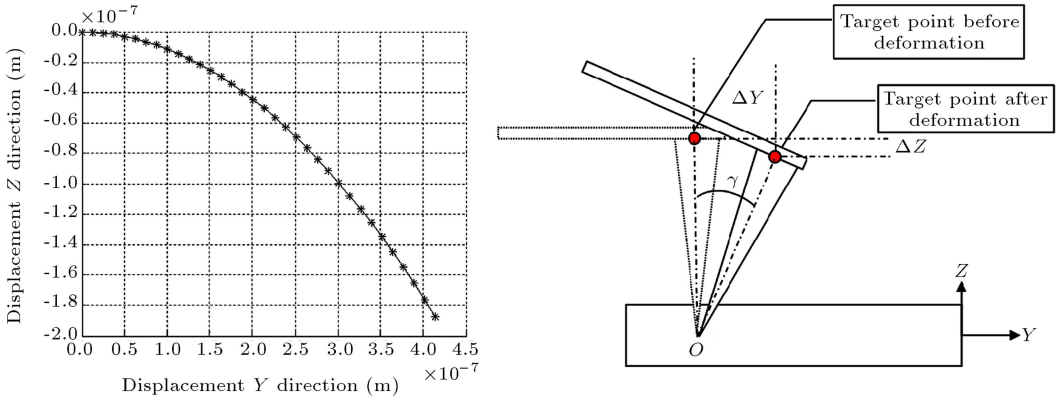

Figure 10. Simulation of target point before departure in Y and Z directions.

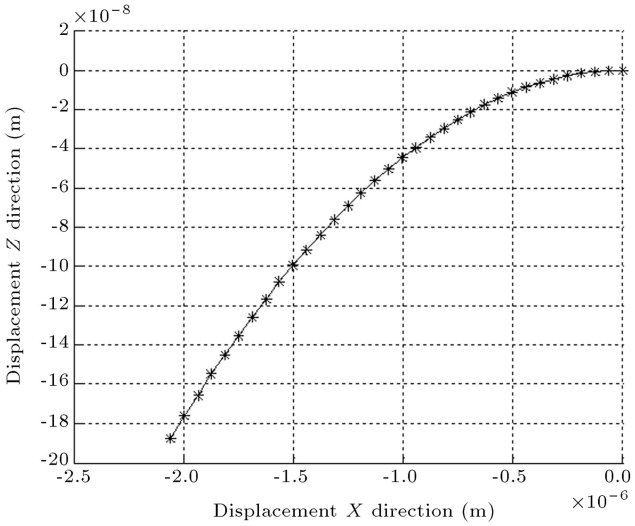

Figure 11. Simulation of target point before departure in X and Z directions.

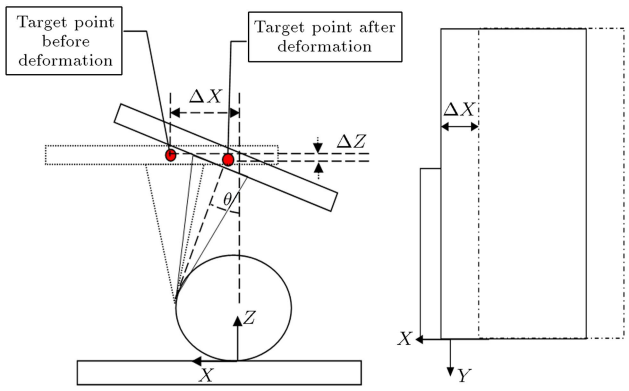

Figure 12. Illustration of target point before departure in X and Z directions.

In the third case, particle spinning is investigated. First, the cantilever has deformed due to applied forces. Then, the cylindrical particle starts to spin relative to substrate speed, and its spin is formulated using the rotation angle, λ. According to the presented model, particle displacement in the X and Y directions increases, as shown in Figures 15 and 16. The negative value is due to the target point's incremental displacement.

5. Verification of the 3D kinematics used for the manipulation of cylindrical nanoparticles

To verify the set up we have used, we refer to [16,17]. In the verification process, a 2D model, which has been applied for spherical particle manipulation, is compared with the proposed 3D model intended for the manipulation of cylindrical nanoparticles. First, the 2D model is introduced. In the 2D model, the distance between fixed coordinates and moving coordinates is indicated by X_s, Y_s and Z_s. Also, as a result of having the same origin in the X and Z directions, the initial values of X_s and Z_s are zero. In the simulation algorithm (Figure 17), R_p is the particle radius, ϕ is the contact angle, θ is the tip's twist angle and H is the cantilever height. Deformations due to contact forces are denoted by δ_s and δ_t for particle-substrate and particle-tip contacts, respectively.

The presented parameters are divided into two types. The first type, consisting of X_s, Y_s, Z_s, R_p, H, ϕ, remains constant during the manipulation process; and the second type, which is time dependent, includes the cantilever's twist angle (θ), and also δ_s and δ_t (as the particle's elastic deformation parameters). The model we have used is detailed in Tafazzoli's work [16,17].

The algorithm is divided into two parts. On the left side of the algorithm, first, the constants are introduced into the simulation process. Also, since the origins of the fixed and moving coordinates are the same, the values of X_s and Z_s are set to zero. The twist angle (θ) is obtained from the diagram of Figure 18, based on Tafazzoli's model. Also, δ_s and δ_t (particle's elastic deformation parameters) are determined using the diagram in Figure 18 [16,17]. The normal force is obtained using the twist angle in the simulation.

Table 2. Constant parameters of the simulation.

Cantilever parameter	Process parameters		Particle geometry	
Probe height, H	**Contact angle, ϕ**	**Spin angle, λ**	**Cylinder length, L**	**Cylinder radius, R_P**
$H = 12\ \mu$m	$\phi = 45^\circ$	$\lambda = 0$	$L = 1\ \mu$m	$R_P = 50$ nm

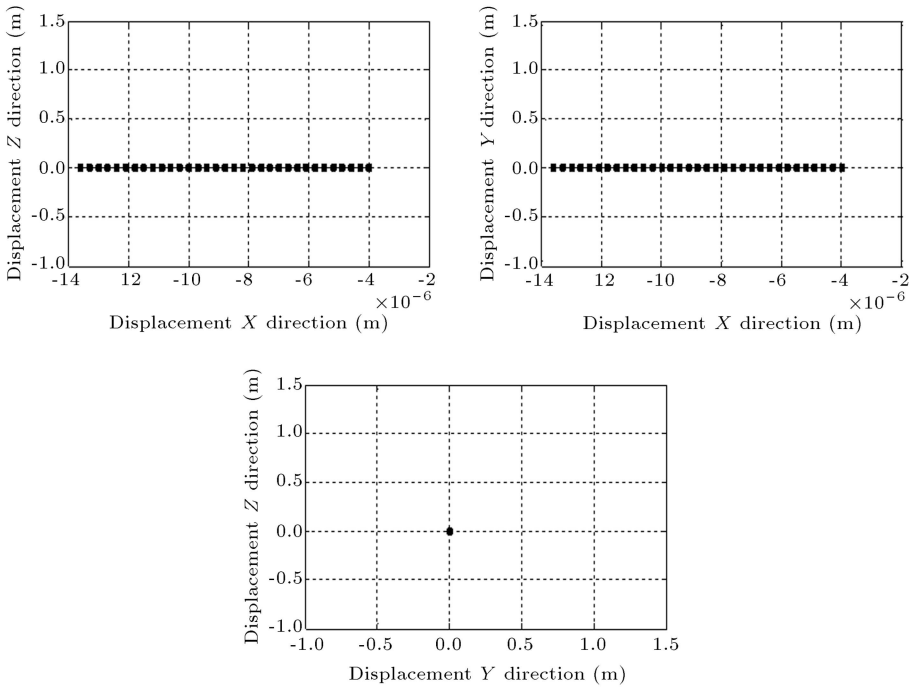

Figure 13. Simulation of sliding and rolling displacements during the manipulation.

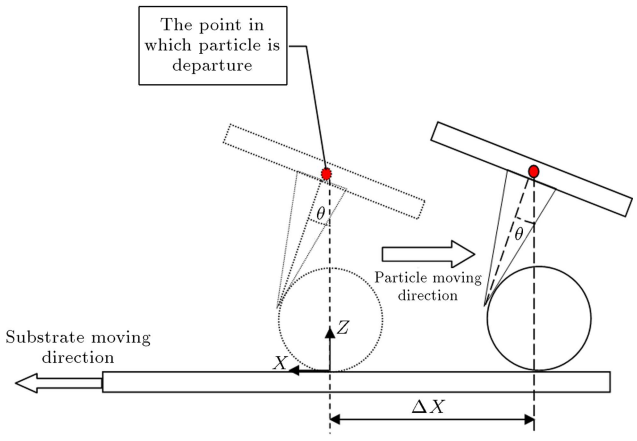

Figure 14. Simulation of particle displacement after departure in the rolling and sliding modes.

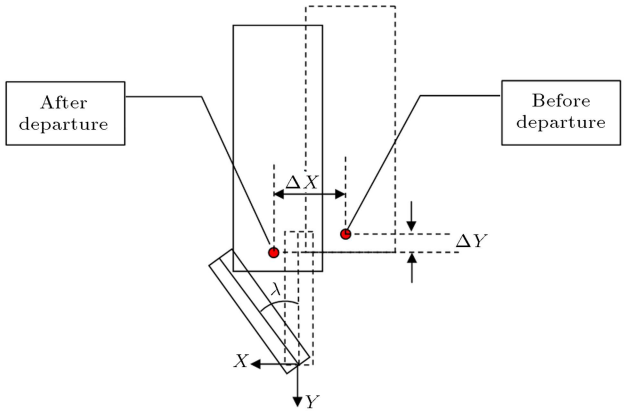

Figure 15. Simulation of particle displacement after departure in the spinning mode.

Finally, our simulation method practically becomes the same as the one proposed by Tafazzoli. Applying this method and using the mentioned parameters, the manipulation kinematics of a spherical nanoparticle is ultimately demonstrated (Figure 19).

The manipulation of a cylindrical nanoparticle is similarly determined. Using Tables 1 and 2, the constant parameters are obtained. The twist angle (θ) and normal force are also determined using the presented model. Using the cylindrical elastic deformation equations (Eqs. (6) to (11)), the particle's elastic deformations (δ_t,δ_s) are obtained, and, by using the constant and variable parameter values, the kinematic model is achieved. As Figure 20 clearly shows, deviation between the two diagrams is very small.

The displacement in the Y direction, which only occurs in 3D kinematics, is eliminated by reducing the effect of 3D parameters, as shown in Figure 20. The

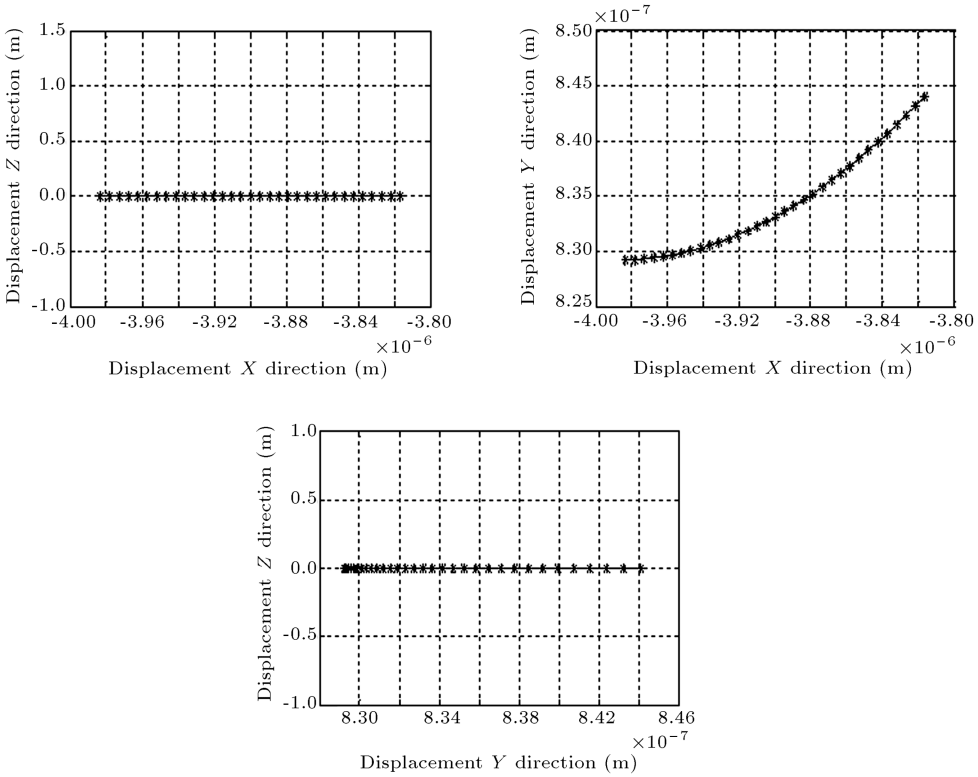

Figure 16. Simulation of spinning displacements during the manipulation.

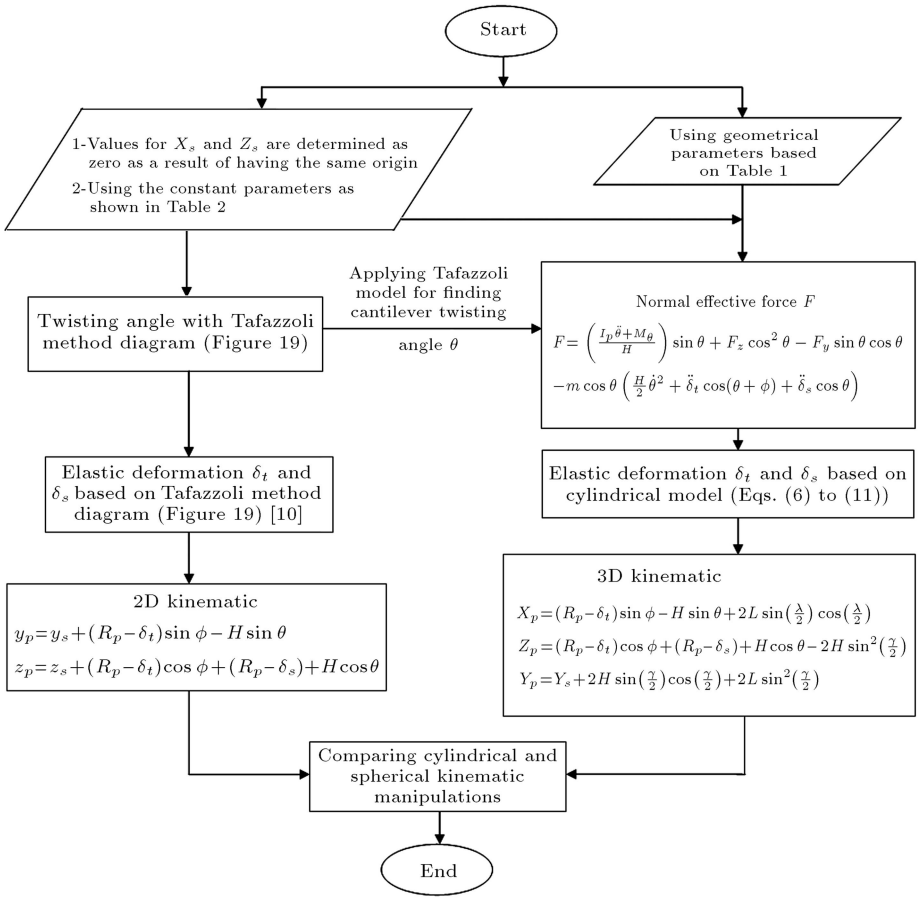

Figure 17. Verification of the algorithm for the manipulation of cylindrical nanoparticles.

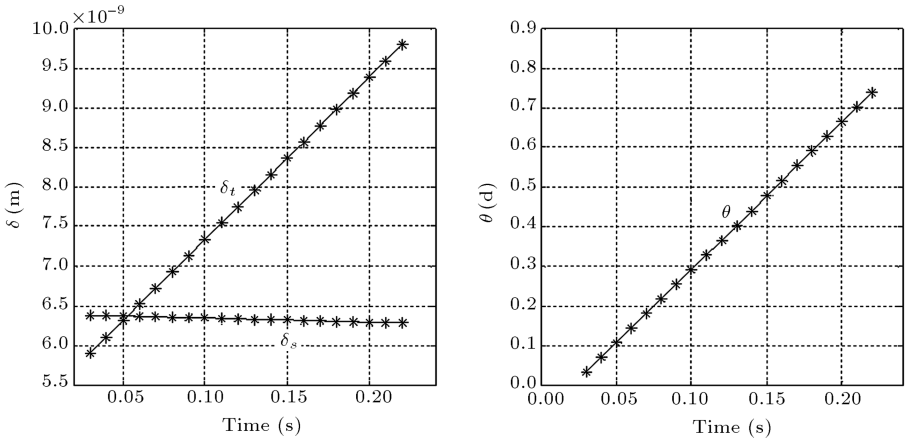

Figure 18. Particle's elastic deformations δ_t and δ_s (left) and the twist angle variation based on Tafazzoli's method [10] (right).

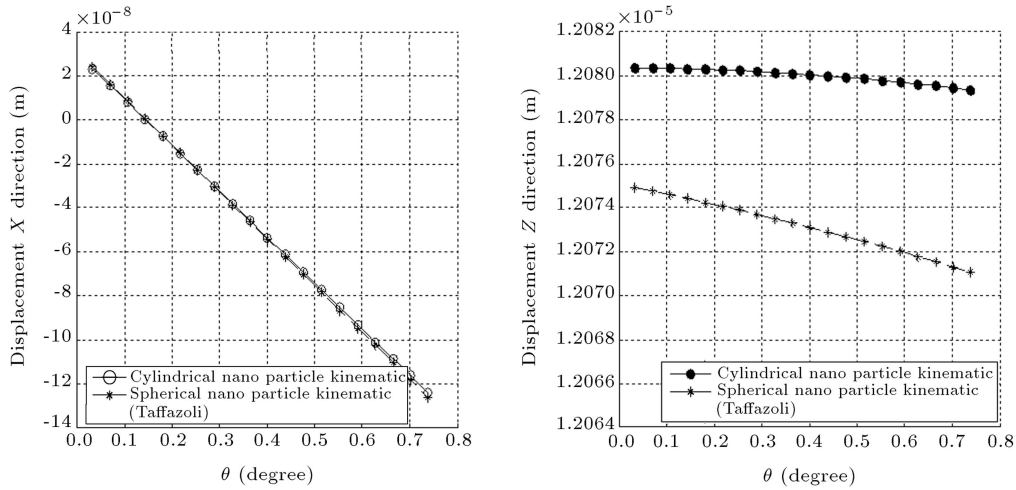

Figure 19. Deviation between the existing 2D simulation and the presented 3D simulation in the X and Z directions.

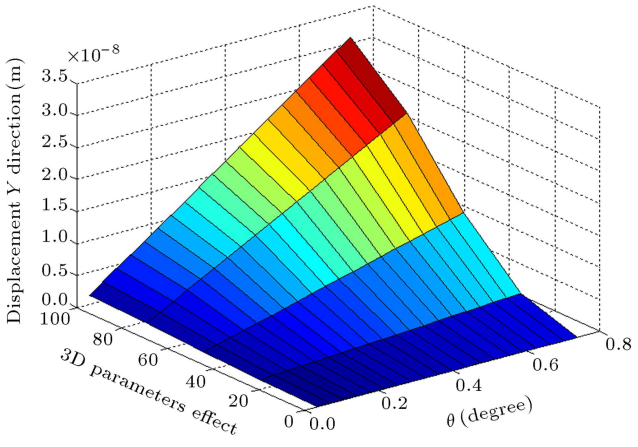

Figure 20. Elimination of displacement in the Y direction as a result of reducing the 3D parameters.

deviation in the X and Y directions is due to using different deformation models in the simulations. In conclusion, using analytical methods and simulations, and through comparison with the existing 2D simulations, the 3D model is validated.

6. Conclusion

Our research underlined the importance of 3D kinematics in nanoparticle manipulation processes. The represented models make it possible to predict the kinematics of nano scale manipulation processes through computational simulations. In this model, it is also possible to predict particle displacements during the manipulation process. Moreover, the 3D capability of the model makes it possible to consider all the probable displacement and motion modes. The introduced model and the related algorithm could be used as a tool to determine particle positioning during the manipulation process. These simulations provide a clear image of the manipulation process.

The presented model makes it possible to determine the displacement, velocity and acceleration of cylindrical particles during positioning by AFM nanorobots. Also, the modeling can help improve the precision of particle positioning. Moreover, this kinematic model provides the first step in the development of a fully-fledged dynamic model.

During the time in which the particle is stuck into the substrate, a deformation of 1.2×10^{-5} is observed in the Z direction, which is basically due to the force applied to the tip-particle contact area. However, the curve of displacement variation in the Z direction, as a result of applying a constant force, does not have a sharp slope (1.5%). In this simulation, the main objective is displacement in the X direction. The X direction displacement starts from zero and reaches a value of 4.14×10^{-5} in its final position. Displacement in the Y direction is similar to that in the X direction.

With numerous applications of cylindrical nanoparticles in NEMS and MEMS structures, on the one hand, and the lack of real-time monitoring in the manipulation process, on the other, kinematic modeling and simulation becomes highly important. Besides, this type of modeling plays a great role in the improvement of the manipulation process at an industrial level, which needs higher automation capability for a practical manufacturing approach.

References

1. Korayem, M.H., Zakeri, M. and Taheri, M. "Simulation of two-dimensional nanomanipulation of particles based on the HK and LuGre friction models", *Arabian Journal for Science and Engineering*, **38**(6), pp. 1573-1585 (2013).
2. Babahosseini, H., Mahboobi, S.H. and Meghdari, A. "Dynamic modeling of a spherical nanoparticle manipulation by atomic force microscope probe", *Journal of Nanoengineering and Nanomanufacturing*, **3**(2), pp. 98-106 (2013).
3. Korayem, M.H. and Hoshiar, A.K. "Modeling and simulation of dynamic modes in the manipulation of nanorods", *Micro & Nano Letters*, **8**(6), pp. 284-287 (2013).
4. Korayem, M.H. and Zakeri, M. "Sensitivity analysis of nanoparticles pushing critical conditions in 2-D controlled nanomanipulation based on AFM", *International Journal of Advanced Manufacturing Technology*, **41**(7-8), pp. 714-726 (2009).
5. Gnecco, E., Rao, A., Mougin, K., Chandrasekar, G. and Meyer, E. "Controlled manipulation of rigid nanorods by atomic force microscopy", *Nanotechnology*, **21**(21), pp. 215702-215707 (2010).
6. Tranvouez, E., Orieux, A., Boer-Duchemin, E., Devillers, C.H., Huc, V., Comtet, G. and Dujardin, G. "Manipulation of cadmium selenide nanorods with an atomic force microscope", *Nanotechnology*, **20**(16), pp. 165304-165314 (2009).
7. Sitti, M. and Hashimoto, H. "Controlled pushing of nanoparticles: modeling and experiments", *IEEE/ASME Transactions on Mechatronics*, **5**(2), pp. 199-211 (2000).
8. Falvo, M.R., Steele, J., Taylor II, R.M. and Superfine, R. "Gearlike rolling motion mediated by commensurate contact: carbon nanotubes on HOPG", *Physical Review B*, **62**(16), pp. 10665-10667 (2000).
9. Xie, H., Régnier, S., "High-efficiency automated nanomanipulation with parallel imaging/manipulation force microscopy", *IEEE Transactions on Nanotechnology*, **11**(1), pp. 21-33 (2012).
10. Junno, T., Deppert, K., Montelius, L. and Samuelson, L. "Controlled manipulation of nanoparticles with an atomic force microscope", *Physical Review Letters*, **66**(26), pp. 3627-3629 (1995).
11. Wong, E.W., Sheehan, P.E. and Lieber, Ch.M. "Nanobeam mechanics: elasticity, strength, and toughness of nanorods and nanotubes", *Science*, **277**(5334), pp. 1971-1975 (1997).
12. Hertel, T., Martel, R. and Avouris, Ph. "Manipulation of individual carbon nanotubes and their interaction with surfaces", *Journal of Physical Chemistry B*, **102**(6), pp. 910-915 (1998).
13. Gnecco, E., Rao, A., Mougin, K., Chandrasekar, G. and Meyer, E. "Controlled manipulation of rigid nanorods by atomic force microscopy", *Nanotechnology*, **21**(21), pp. 215702-215707 (2010).
14. Conache, G., Gray, S., Bordag, M., Ribayrol, A., Fröberg, L.E., Samuelson, L., Pettersson, H. and Montelius, L. "AFM-based manipulation of inas nanowires", *Journal of Physics: Conference Series*, **100**(5), pp. 052051-052054 (2008).
15. Falvo, M.R., Clary, G., Helser, A., Paulson, S., Taylor II, R.M., Chi, V., Brooks F.P. Jr., Washburn, S. and Superfine, R. "Nanomanipulation experiments exploring frictional and mechanical properties of carbon nanotubes", *Microscopy and Microanalysis*, **4**(5), pp. 504-512 (1999).
16. Tafazzoli, A. and Sitti, M. "Dynamic behavior and simulation of nanoparticles sliding during nanoprobe-based positioning", *International Mechanical Engineering Congress (ASME)*, Anaheim, pp. 965-972 (2004).
17. Tafazzoli, A. and Sitti, M. "Dynamic modes of nanoparticle motion during nanoprobe-based manipulation", *IEEE Nanotechnology Conference*, Germany, pp. 35-37 (2004).
18. Korayem, M.H., Hoshiar, A.K. and Ebrahimi, N. "Maximum allowable load of Atomic Force Microscope (AFM) nanorobot", *International Journal of Advanced Manufacturing Technology*, **43**(7-8), pp. 690-700 (2009).
19. Korayem, M.H. and Zakeri, M. "The effect of off-end tip distance on the nanomanipulation based on rectangular and V-shape cantilevered AFMs ", *International Journal of Advanced Manufacturing Technology*, **50**(5-6), pp. 579-589 (2010).
20. Korayem, M.H., Zakeri, M. and Aslzaeim, M. "Sensitivity analysis of the nanoparticles on substrates using

the atomic force microscope with rectangular and V-shaped cantilevers", *Micro & Nano Letters*, **6**(8), pp. 586-591 (2011).

21. Zhang, J., Li, G. and Xi, N. "Modeling and control of active end effector for the AFM based nano robotic manipulators", *International Conference on Robotics and Automation (ICRA-IEEE)*, Spain, pp. 163-168 (2005).
22. Moradi, M., Fereidon, A.H. and Sadeghzadeh, S. "Aspect ratio and dimension effects on nanorod manipulation by atomic force microscope", *Micro & Nano Letters*, **5**(5), pp. 324-327 (2010).
23. Korayem, M.H. and Hoshiar, A.K. "Dynamic 3D modeling and simulation of nanoparticles manipulation using an AFM nanorobot", *Robotica*, Available on Line 08 October 2013, pp. 1-17 (2013).
24. Hsu, J.H. and Chang, S.H. "Tribological interaction between multi-walled carbon nanotubes and silica surface using lateral force microscopy", *Wear*, **266**(9-10), pp. 952-959 (2009).
25. Hertz, H.R. "Ueber die Beruehrung elastischer koerper (on contact between elastic bodies)", In *Gesammelte Werke (Collected Works)*, **1**(1), pp. 156-160 (1895).
26. Johnson, K.L., Kendall, K. and Roberts, A.D. "Surface energy and the contact of elastic solids", *Proceedings of the Royal Society of London A*, **324**(1558), pp. 301-313 (1971).
27. Barquins, M. "Adherence, friction and wear of rubber-like materials", *Wear*, **158**(1-2), pp. 87-117 (1992).
28. Pocius, A.V., *Surfaces, Chemistry and Applications: Adhesion Science and Engineering*, Elsevier, pp. 81-91 (2002).

Biographies

Moharam Habibnejad Korayem was born in Tehran, Iran, in 1961. He received his BS (Hon) and MS degrees in Mechanical Engineering from Amirkabir University of Technology, Tehran, Iran, in 1985 and 1987, respectively, and his PhD degree in Mechanical Engineering from the University of Wollongong, Australia, in 1994. He is currently Professor of Mechanical Engineering at Iran University of Science and Technology, where he has been involved in teaching and research activities in the area of robotics for the last 19 years. His research interests include dynamics of elastic mechanical manipulators, trajectory optimization, symbolic modeling, robotic multimedia software, mobile robots, industrial robotics standard, robot vision, soccer robot, and the analysis of mechanical manipulators with maximum load carrying capacity. He has published more than 500 papers in international journals and conferences in these areas.

Ali Kafash Hoshiar was born in Tehran, Iran, in 1981. He received his BS degree in Mechanical Engineering from Islamic Azad University, Central Tehran Branch, in 2004, and his MS degree, in the field of nano robotics, in 2007, from Islamic Azad University, Science and Research Branch, where he is currently a PhD degree candidate in the same field. Three ISI papers and several accepted conferences are the results of his research so far. His research interests include robotic systems, atomic force microscopy dynamics, sensitivity analysis, nano manipulators and micro-nano robots.